Atmospheric Research 230 (2019) 104631

Contents lists available at ScienceDirect

Atmospheric Research

journal homepage: www.elsevier.com/locate/atmosres

Secondary organic aerosol formation from α-methylstyrene atmospheric degradation: Role of NO_x level, relative humidity and inorganic seed aerosol

Mercedes Tajuelo[a], Ana Rodríguez[a,*], María Teresa Baeza-Romero[b], Alfonso Aranda[c], Yolanda Díaz-de-Mera[c], Diana Rodríguez[a]

[a] University of Castilla La Mancha, Faculty of Environmental Sciences and Biochemistry, Avenida Carlos III, s/n, 45071 Toledo, Spain
[b] University of Castilla La Mancha, School of Industrial Engineering, Avenida Carlos III, s/n, 45071 Toledo, Spain
[c] University of Castilla La Mancha, Faculty of Chemical Sciences, Avenida Camilo José Cela 10, 13071 Ciudad Real, Spain

ARTICLE INFO

Keywords:
α-Methylstyrene
SOA
NOx
Relative humidity
Inorganic seed aerosols

ABSTRACT

Secondary Organic Aerosol (SOA) formation during the photolysis and OH-photooxidation of α-methylstyrene was investigated using a simulation chamber at atmospheric pressure and room temperature (296 ± 1) K. α-Methylstyrene concentration was followed by gas chromatography with a mass spectrometric detector (GC–MS) and the aerosol production was monitored using a Fast Mobility Particle Sizer (FMPS). The effect of varying α-methylstyrene (0.5 ppm - 2 ppm) and NOx (0.5 ppm - 1.0 ppm) concentrations on SOA formation was explored, as was the effect of the relative humidity (RH) (5–50%) and the presence of inorganic seed particles. Results indicate that SOA yields increase at higher α-methylstyrene concentrations; low NOx and high RH conditions favour more rapid aerosol formation and a higher aerosol yield; SOA formation is independent of seed surface area, within the studied range, for both inorganic seed particles ($(NH_4)_2SO_4$ and $CaCl_2$). An off-line chemical analysis using a filter/denuder sampling system and GC–MS confirms acetophenone as the main gas phase product in both processes, photolysis and photooxidation. For the first time, SOA composition in α-methylstyrene degradation was analysed, observing acetophenone and acetol as products present in the formed aerosol in presence and absence of NOx.

1. Introduction

Organic material significantly contributes ~20–50% to the total fine aerosol mass at continental mid-latitudes and as high as 90% in tropical forested areas (Kanakidou et al., 2005). This organic aerosol consists of primary organic aerosol (POA) emitted directly into the atmosphere and secondary organic aerosol (SOA), which can be either natural or anthropogenic, formed in the atmosphere by gas-particle conversion processes such as nucleation, condensation and heterogeneous chemical reactions (Hallquist et al., 2009). SOA composes up to 80% of all organic aerosols (Zhang et al., 2007) and contribute to the attenuation of regional visibility (Hand and Malm, 2007), climate change (Stocker et al., 2013) and it presents potential health hazards (Pope and Dockery, 2006). However, the chemistry and physics of SOA are poorly understood, and, despite significant efforts, model-predicted atmospheric SOA loadings are consistently and significantly different from field-measured loadings (Kanakidou et al., 2005; Zhang et al., 2007; Kroll and Seinfeld, 2008; Gouw and Jimenez, 2009; Dzepina et al., 2009).

Among the various organic compounds, aromatic hydrocarbons are one of the types of organic aerosol precursors which have drawn the most attention due to their abundance in the air and their high SOA contribution in urban atmospheres (Lewandowski et al., 2008; Yuan et al., 2013). In this sense, styrene and its derivatives, including α-methylstyrene are aromatic compounds present in polluted areas (Okada et al., 2012; Knighton et al., 2012; Gentner et al., 2013; Zhang et al., 2017), potentially leading to SOA and photochemical ozone formation (Diaz-de-Mera et al., 2017; Berezina et al., 2017; Tajuelo et al., 2019a). α-Methylstyrene emissions come from its use in the industry, since it is used to improve the hardness and resistance of polymers against high temperatures, mainly in plastics, rubbers and coatings (Lewis et al., 1983). Other uses of α-methylstyrene include applications in musk oil fragrances, plasticizers in paints, waxes and adhesives (Santodonato et al., 1980). The International Agency for Cancer Research (IARC (International Agency of Research for Cancer), 2019) has classified it as possible carcinogenic to humans, based on results of experimental inhalation studies in which enough evidence for carcinogenicity was found in animals (NTP (National Toxicology

* Corresponding author.
E-mail address: Anamaria.rodriguez@uclm.es (A. Rodríguez).

https://doi.org/10.1016/j.atmosres.2019.104631
Received 28 May 2019; Received in revised form 17 July 2019; Accepted 22 July 2019
Available online 24 July 2019
0169-8095/

Programa), 2007). Once in the atmosphere, α-methylstyrene can be degraded by oxidation with the main tropospheric oxidants, although its dominant atmospheric loss process is clearly its reaction with OH radical (Tajuelo et al., 2019b). These reactions give rise to gas phase products (Bignozzi et al., 1981; Le Person et al., 2008; Tajuelo et al., 2019b), but SOA formation is also expected, since the aerosol formation from the styrene photolysis and oxidation with OH radicals and ozone has been reported previously (Diaz-de-Mera et al., 2017; Tajuelo et al., 2019a), and both compounds are structurally similar.

SOA formation is strongly dependent on the environmental conditions under which this aerosol is formed. Inorganic and organic mass loading, particle acidity, NOx (NO and NO_2) level and relative humidity (RH) affect the SOA yields and their composition. In this way, the level of NOx has been found to be highly influential in SOA formation from a variety of compounds. Generally, a higher SOA yield is observed under low-NOx conditions, although this fact changes dependent on the precursor organic compound (Ng et al., 2007a; Ng et al., 2007b; Kleindienst et al., 2012; Li et al., 2014; Sarrafzadeh et al., 2016). Water plays also an important role in the formation of SOA in aromatic compounds photooxidation. Numerous studies about the humidity effect on SOA formation have been carried out, in which positive, negative and even non-significant effects have been observed dependent on the organic precursor considered. (Cocker III et al., 2001; Healy et al., 2009; Jia and Xu, 2010; Kamens et al., 2011; Zhou et al., 2011; Jia and Xu, 2014). The same applies to the influence of inorganic seeds on SOA mass yields, where again contradictory results are found (Zhou et al., 2011; Kamens et al., 2011; Zhang et al., 2012; Huang et al., 2017). One of the reasons to account for the discrepancies among different studies is the surface area of seeds. This factor is important due to competition for SOA-forming vapour deposition between the chamber wall and the seed particles (Huang et al., 2017).

Therefore, it is crucial to explore SOA formation mechanisms from anthropogenic precursors, analysing the effect of different NOx, RH and seed particles levels. For this reason, this study aims at (i) analysing for the first time the possible formation of SOA from α-methylstyrene atmospheric oxidation, both by photolysis and by photooxidation with hydroxyl (OH) radicals; (ii) investigating the role of NOx, RH and inorganic seed particles presence on this formation; (ii) characterizing the chemical composition of the products obtained in above processes, both in gas and particulate phase. The results obtained in this work might be used in air quality models representing different environmental conditions.

2. Experimental section

Four different types of experiments were performed in this study, each with different objectives. The first type is the reference experiment, which consisted in observing SOA formation from α-methylstyrene photolysis and its photooxidation with OH radicals, in the absence of NOx and low RH at variable α-methylstyrene initial concentration. The results of this type of experiment will be compared with the rest of experiments. The second type of experiment was performed in presence of water vapour to analyse the differences in the SOA formation induced by the particle liquid water content. For the third type of experiment, NOx was introduced into the smog chamber, and provided additional insight into the impact of NOx on SOA formation. Finally, inorganic seed particles, in particular $(NH_4)_2SO_4$ and $CaCl_2$, were introduced into the chamber to act as substrates onto which the gas-phase products may condense.

2.1. Chamber experiments

The experimental system and the procedures used in this work have been described at great length previously (Tajuelo et al., 2019a). Only details relevant to the present study are briefly described below. Experiments were performed in a 500 L Teflon bag housed in an isothermal cabinet with six fluorescent lamps (Philips TUV G13, 36 W) mounted on the walls, under room temperature and atmospheric pressure.

A previous study with only α-methylstyrene/air samples in the reactor showed that wall losses were negligible (Tajuelo et al., 2019b). Before each experiment, the chamber was cleaned with synthetic air (99.999%, Praxair) until the particle number concentration was < 20 particles cm^{-3}, which are completely negligible compared to the SOA concentrations formed from α-methylstyrene. In absence of NOx, a known volume of high-purity liquid α-methylstyrene (99%, Sigma-Aldrich) was injected into the chamber and flushed with a flow of synthetic air, both in photolysis and photooxidation experiments. In photooxidation experiments, OH radicals were generated by photolysis (λ = 254 nm) of H_2O_2 (60%, Fisher Scientific). The initial concentrations of H_2O_2, when it was injected, and α-methylstyrene were 2 ppm and 0.25–2 ppm, respectively. Before irradiation, the Teflon bag was maintained in the dark for 1 h for the reactants to get mixed thoroughly. OH concentrations were estimated from the measured α-methylstyrene decay and the literature rate constant ($k_{OH+\ \alpha\text{-methylstyrene}} = (5.3 \pm 0.6) \times 10^{-11}\ cm^3\ molecule^{-1}\ s^{-1}$) (Bignozzi et al., 1981). The calculated average OH radical concentration (3.4×10^6 molecules cm^{-3}) is within the same magnitude of the 12 h daytime average OH concentration in the troposphere (Hein et al., 1997).

To analyse the humidity effect on the SOA formation from α-methylstyrene, water vapour was generated using a glass bubbler placed just before the reactor inlet. The amount of water required for a given RH was calculated and injected into the bubbler. The water was then evaporated and flushed inside the reactor using synthetic air. RH was varied in the experiments between 5% and 50%.

For experiments in presence of NOx, NO was introduced by flushing pure N_2 (99.999%, Praxair) through a calibrated glass bulb filled to a predetermined partial pressure of pure NO (Linde, 99.5%). α-Methylstyrene, H_2O_2 in photooxidation experiments, and NO were injected and well mixed before lights were turned on to start the experiment. Typical concentrations in these conditions were: α-methylstyrene = 0.5 or 2.0 ppm; H_2O_2 = 2 ppm and NO = 1 ppm.

To investigate the seed aerosol effect on the growth of the SOA formed from α-methylstyrene photolysis and photooxidation, $(NH_4)_2SO_4$ (99%, Sigma) and $CaCl_2$ (97%, Sigma) were selected as neutral and acid inorganic salt, respectively. $CaCl_2$ is one of the major inorganic aerosol species during dust days, while $(NH_4)_2SO_4$ is a major constituent during haze days (Wang et al., 2006). These seeds were produced by aspirating a 0.01 mol/L salt solution through a constant output atomizer (TSI Inc., 3076), which were subsequently passed through a diffusion dryer (TSI Inc., 3062) to decrease the humidity below 12%. The initial seed concentrations in the chamber ranged between 3000 and 10,0000 particles cm^{-3}, with a diameter of 50 to 80 nm.

2.2. Gas and particle phase measurements

α-Methylstyrene concentration was continuously monitored by gas chromatography–mass spectrometric detection (GC–MS, Shimadzu QP2010), using a capillary column (size: 30 m × 0.32 mm × 1 m, Meta X5 Teknokroma) maintained isothermally at 125 °C. RH, temperature and NOx, were also monitored. The RH was measured by a humidity sensor (Vaisala, HMT333). Without added water vapour, RH was ~ 5%. The temperature was relatively constant at 20 °C (Crison, TM65) before the experiments start and increased to a stable value of approximately 23 °C after the lamps were turned on. NOx concentrations were measured with a chemiluminescence analyser (Environnement, AC3 2 M).

The formation of particles was followed by a fast mobility particle sizer (FMPS) (TSI Inc., 3091) to obtain the particle size distribution and total mass of particles with diameters within the range 5.6–560 nm (Aranda et al., 2015). The total aerosol mass concentration was calculated from the measured particle size distribution assuming unit density

and spherical particles. All experiments were conducted until the aerosol mass was constant, corresponding to approximately 4–5 h of irradiation. The initial mass present in the reactor was measured before turning on the lamps, thus the aerosol mass concentration (M_o) was calculated by subtracting the initial mass to the final mass. In the absence of NOx, aerosol seeds and low RH, the level of particles was below 20 particles cm^{-3}.

To determine the SOA wall loss rates, the lamps were turned off at the end of the reaction and the aerosols were measured over a period of 1–2 h. The average loss rate of the total aerosol mass is measured from a first-order decay. This method is effective in experiments that use low seed aerosol surface area concentrations ($< 3000\ \mu m^2\ cm^{-3}$) and the coagulation is negligible (Nah et al., 2017).

The gas- and particle-phase products formed in the photolysis and photooxidation of α-methylstyrene were analysed by an off-line analytical method. Thus, to collect the gas and particle phase products separately, a denuder/filter system was used, which was made up of a 242 mm, 5-channel XAD4-coated annular denuder, a prebaked (500 °C for 12 h), 47 mm quartz fibre filter (Whatman 1851–047 QMA) and a sampling pump at 25 L min^{-1}, all in series. The contents of the denuder and filter were extracted using two 10 mL portions of methanol and derivatized with O-(2,3,4,5,6-Pentafluorobenzyl) hydroxylamine hydrochloride (PFBHA) (99%, Sigma). Then, 1 mL from each extract was filtered using a PTFE membrane filter (pore size 0.45 μm) and reduced under a nitrogen stream almost to dryness and reconstituted with n-hexane (Acros Organics, > 97%). The extracts of both the gas (from denuder) and particle phase (from filter) were analysed by GC–MS. A detailed description of all the process has been previously published (Tajuelo et al., 2019a).

3. Result and discussion

3.1. Aerosol formation

Table 1 summarizes the initial conditions for all experiments, as well as the averaged results of at least two experiments for each experimental condition.

Fig. 1 shows typical concentration-time profiles (corrected for wall-loss correction) obtained for α-methylstyrene in a reference experiment, with low NOx (< 12 ppb) and RH level (< 6%), both in the photolysis and photooxidation. Particle formation was not observed until ~35 min (photolysis) and ~12 min (photooxidation) of the start of the reaction, with a fast increase in the particle number concentration followed by a gradual decrease after reaching a maximum at 60 and 45 min for photolysis and photooxidation, respectively. This observation is consistent with an initial nucleation step producing a burst of nanoparticles, followed by coagulation which results in an increase in the mass of the particle, along with a corresponding decrease in the number. After 5–6 h, SOA mass concentration reaches a plateau which is consistent with slower rate of reaction due to the reduction of the precursor concentrations. Moreover, the aerosol mass concentration formed by photooxidation is higher than by photolysis, thus the SOA formation is enhanced in presence of OH radicals.

Regarding the evolution of the particle size distributions with the reaction time (see Fig. S1), the initial particles observed were very small, with diameters starting around 7 nm, but they grew up fast until a final maximum diameter of around 220 nm for the photolysis and 400 nm for the photooxidation. Due to its size, these kinds of particles can be inhaled, reaching the lungs and causing serious health effects (Breitner et al., 2011).

3.2. Effect α-methylstyrene initial concentration

A series of experiments were carried out to assess the effect of initial α-methylstyrene concentration on the SOA formation. Table 1 shows the results obtained in the maximum particle number concentration and aerosol mass concentration varying α-methylstyrene concentrations from 250 to 2000 ppb. Both in photolysis and in photooxidation experiments, the particle number and their growth were larger for higher α-methylstyrene concentrations.

The overall organic aerosol yield (Y) was determined experimentally as the ratio of organic aerosol mass concentration (Mo) to the mass of the parent organic species consumed at the end of each experiment:

$$Y = \frac{M_0}{\Delta[\alpha - methylstyrene]} \quad (1)$$

The measured aerosol mass concentration had to be corrected in each experiment for wall losses. The method has been described previously (Tajuelo et al., 2019a), where the first order particle-wall deposition rate used was $(1.10 \pm 0.85) \times 10^{-3}\ min^{-1}$. The average corrected Mo and the corresponding Y are reported in Table 1.

The data suggest again that the aerosol formation is affected by the initial concentration of the organic precursor, with higher initial α-methylstyrene concentrations leading to higher SOA yields. This result is in accordance with reactivity, as increasing the initial hydrocarbon concentration leads to the formation of a higher number of condensable products and thus higher SOA mass concentration. Moreover, as the organic aerosol mass directly affects the gas/particle partitioning by acting as the medium into which oxidation product can be absorbed, higher SOA mass leads to higher SOA yields.

SOA yields can be described by a widely-used semi-empirical model based on absorptive gas-particle partitioning of semivolatile products (Odum et al., 1996) in which Y of a particular hydrocarbon is given by:

$$Y = M_0 \sum_i \left(\frac{\alpha_i K_{om,i}}{1 + K_{om,i} M_0} \right) \quad (2)$$

where α_i is the mass-based stoichiometric coefficient of semi-volatile product i and $K_{om,i}$ is the gas-particle partitioning equilibrium constant. Generally, a one-product model has been proved sufficiently accurate to describe the relationship between aerosol yield and mass (Tajuelo et al., 2019a; Ng et al., 2007b; Lauraguais et al., 2012; Liu et al., 2019). In this way, experimental data were fitted to Eq. (2) (see Fig. S2), resulting the following parameters: $\alpha_i = (3.05 \pm 0.05) \times 10^{-2}$ and $K_{om,i} = (1.03 \pm 0.14) \times 10^{-1}\ m^3\ \mu g^{-1}$ for the photolysis; and $\alpha_i = (4.54 \pm 0.08) \times 10^{-2}$ and $K_{om,i} = (5.78 \pm 0.78) \times 10^{-2}\ m^3\ \mu g^{-1}$ for the photooxidation with OH radicals.

Moreover, the validity of the approach of using the one-product model was confirmed by plotting M_0 vs. consumed α-methylstyrene concentration, since a linear dependence between both would indicate that one-product model fits the SOA formation (Ng et al., 2006; Ahmad et al., 2017). As shown Fig. 2, a good linear regression fit was obtained for both processes, with a slope of $(3.08 \pm 0.06) \times 10^{-2}$ and $(4.36 \pm 0.09) \times 10^{-2}$ for the photolysis and photooxidation, respectively, which seem to correspond to high-limit aerosol yields. As these values and α_i are very close, this suggests that the low-volatility compounds formed in the reaction of α-methylstyrene degradation are transferred almost completely into the particle phase (Coeur-Tourneur et al., 2010).

SOA yields determined in this work and the results of the fittings (Fig. 2 and Fig. S2) can be compared with those reported in our previous work for the photolysis and OH-photooxidation of styrene (Tajuelo et al., 2019a). In both cases and for the same experimental conditions (2 ppm of the hydrocarbon and low NOx and RH levels), SOA yields measured for α-methylstyrene (2.8 and 4.3 for photolysis and photooxidation, respectively) are slightly lower than those of styrene (3.5 (photolysis) and 5.0 (photooxidation)). Generally, the additional methyl groups in organic compounds decrease the vapour pressure. Therefore, the vapour pressures of oxygenated products of α-methylstyrene would be lower than those from styrene, and higher SOA yields are expected for α-methylstyrene than for styrene. However, this is opposite to observations from our experiments and other studies

Table 1
Experimental conditions and averaged summary of the results. The uncertainties of SOA yields are the standard deviations of the calculated yields for replicate experiments.

Exp. description	[AMS][b] (ppb)	RH (%)	$[NO]_0$ (ppb)	$[NO_2]_0$ (ppb)	Particle number × 10^4 (p/cm^3)	Δ[AMS][b] (μg/m^3)	M_0 (μg/m^3)	SOA yield (%)
				Dry and low NOx experiments				
Photolysis	250	5.3	2.6	5.7	3.1	858.2	15.9	1.8 ± 0.2
	350	4.7	2.5	7.3	2.8	1245.4	29.3	2.4 ± 0.5
	500	4.9	2.2	6.9	4.3	2144.6	57.8	2.7 ± 0.3
	750	5.1	2.8	7.9	4.9	3301.0	97.2	2.9 ± 0.1
	1000	5.2	1.9	9.5	5.0	4000.1	112.7	2.8 ± 0.4
	1500	5.4	3.4	9.3	6.0	5925.5	170.0	2.9 ± 0.3
	2000	5.0	2.4	5.7	6.4	8278.7	232.4	2.8 ± 0.2
Photooxidation[a]	250	4.9	3.2	5.1	5.5	1103.9	30.8	2.8 ± 0.2
	350	5.3	3.9	7.5	5.1	1795.4	52.9	3.4 ± 0.3
	500	4.8	2.7	6.2	5.0	2665.9	100.8	4.0 ± 0.5
	750	5.5	2.4	8.9	4.8	3335.1	138.8	4.2 ± 0.3
	1000	5.4	1.9	7.2	4.4	4456.7	171.7	4.0 ± 0.1
	1500	5.5	2.8	6.4	4.8	6602.6	279.2	4.2 ± 0.2
	2000	5.2	3.6	8.1	6.7	8364.3	357.2	4.3 ± 0.3
				Wet experiments with low NOx				
Photolysis	500	25.9	2.5	6.7	4.8	1954.1	74.8	3.8 ± 0.7
	500	48.5	1.4	8.6	7.4	2438.2	138.9	4.3 ± 0.5
	2000	26.3	2.8	7.8	7.7	8084.3	323.7	4.0 ± 0.3
	2000	50.1	3.4	9.5	8.6	8249.3	414.1	5.0 ± 0.6
Photooxidation[a]	500	24.8	1.6	5.8	6.1	2687.1	125.2	4.7 ± 0.1
	500	49.6	2.3	4.9	5.8	2684.4	135.6	5.1 ± 0.4
	2000	25.4	2.7	3.9	9.7	7038.0	385.7	5.5 ± 0.6
	2000	48.1	2.9	3.7	13.0	8417.5	504.3	6.0 ± 0.3
				High NOx experiments in dry conditions				
Photolysis	2000	5.2	888.6	17.2	3.4×10^4	8990.7	223.5	2.5 ± 0.4
Photooxidation[a]	500	5.8	1026.3	153.7	2.5×10^4	2271.7	62.7	2.8 ± 0.5
	2000	5.3	497.1	15.3	3.9×10^4	9143.6	309.1	3.4 ± 0.3
	2000	5.1	898.9	79.6	3.3×10^4	9377.9	276.0	2.9 ± 0.2
				High NOx experiments in wet conditions				
Photolysis	2000	48.7	802.4	37.9	6.1×10^4	8927.5	247.7	2.8 ± 0.4
Photooxidation[a]	500	51.3	922.2	79.0	1.1×10^5	2250.2	78.0	3.5 ± 0.3
	2000	49.5	975.7	105.6	5.2×10^4	9149.1	352.3	3.9 ± 0.5

[a] 2 ppm H_2O_2.
[b] AMS = α-methylstyrene.

about similar compounds (Johnson et al., 2005; Cao and Jang, 2007; Li et al., 2016). This suggests that in addition to the gas–particle partitioning, heterogeneous reactions in the aerosol are an important process for SOA formed from aromatic compounds. This observation can be explained considering that carbonyl compound, aldehydes and ketones, are produced from the gas phase reaction of organic compounds with OH radicals. Both types of compounds are involved in heterogeneous reactions, however, their molecular structures impact heterogeneous SOA growth. In general, aldehydes have higher reactivity and favourable equilibrium constants for formation of hydrates and hemiacetals that are important intermediates for heterogeneous reactions (Carey and Sundberg, 2000). Therefore, aldehydes result in greater SOA yields than ketones. The oxidation of styrene produces more aldehydes (Tajuelo et al., 2019a) leading to higher SOA yields, while the oxidation of α-methylstyrene generates more ketones, as shown in section 3.5, resulting in smaller SOA yields. This behaviour has been observed when comparing ethylbenzene with isopropylbenzene (Li et al., 2016); and toluene with 1,3,5-trimethoxybenzene (Cao and Jang, 2007) in photooxidation experiments under low NOx conditions and dry conditions.

3.3. NOx and humidity effects

Photolysis and photooxidation experiments with different NOx concentrations (low and high conditions) and different RH (dry and wet conditions) were carried out in the absence of inorganic seed aerosols. At low NOx concentration, the RH was changed at ~ 5%, 30% and 50%. At high NOx concentration, the experiments were carried out at ~5% and 50% of RH. Table 1 lists the conditions for these experiments.

At ~5% of RH, dry conditions, in high-NOx conditions, both the mass and the number particles were lower than those at low NOx, indicating NOx suppressed the new particle formation (Table 1). Fig. 3 shows the temporal evolution of α-methylstyrene, NOx and mass particle in these experiments, where SOA formation increased after NO was depleted. Thus, in presence of NOx, the formation of first particles were delayed regarding the same experiment in low NOx conditions.

These observations are in agreement with our findings for styrene (Tajuelo et al., 2019a). NOx level plays a critical role in SOA formation, by governing the reactions of organo-peroxy radicals (RO_2) (Song et al., 2005; Song et al., 2007). As the mechanism shows (Fig. 4), under low-NOx concentration, RO_2 radicals react primarily with HO_2 or with other RO_2 radicals, leading to lower-volatility products and enhancing SOA formation. However, under high NOx conditions, the primary loss process of RO_2 radical is reaction with NO to produce alkoxy radicals (RO) or as a minor pathway, organic nitrates ($RONO_2$). For VOCs with ≤ C10, like α-methylstyrene and styrene, these RO radicals generally fragment into smaller more volatile products, resulting in small amounts of SOA when NOx is present (Presto et al., 2005; Kroll et al., 2006; Kroll et al., 2008).

Regarding RH experiments, comparison of the results (see Table 1), show that the SOA mass yields were found to increase as the RH was raised, as well as the particle number and mass concentration at low NOx.

The photooxidation experiments of many aromatic compounds, such as benzene (Jia and Xu, 2014), toluene (Cao and Jang, 2010; Kamens et al., 2011; Hinks et al., 2018), ethylbenzene (Jia and Xu, 2014), m-xylene (Zhou et al., 2011), 1,3,5-trimethylbenzene (Cocker III et al., 2001) and styrene (Tajuelo et al., 2019a) have been carried out to study the RH effect on SOA formation. The results exhibited

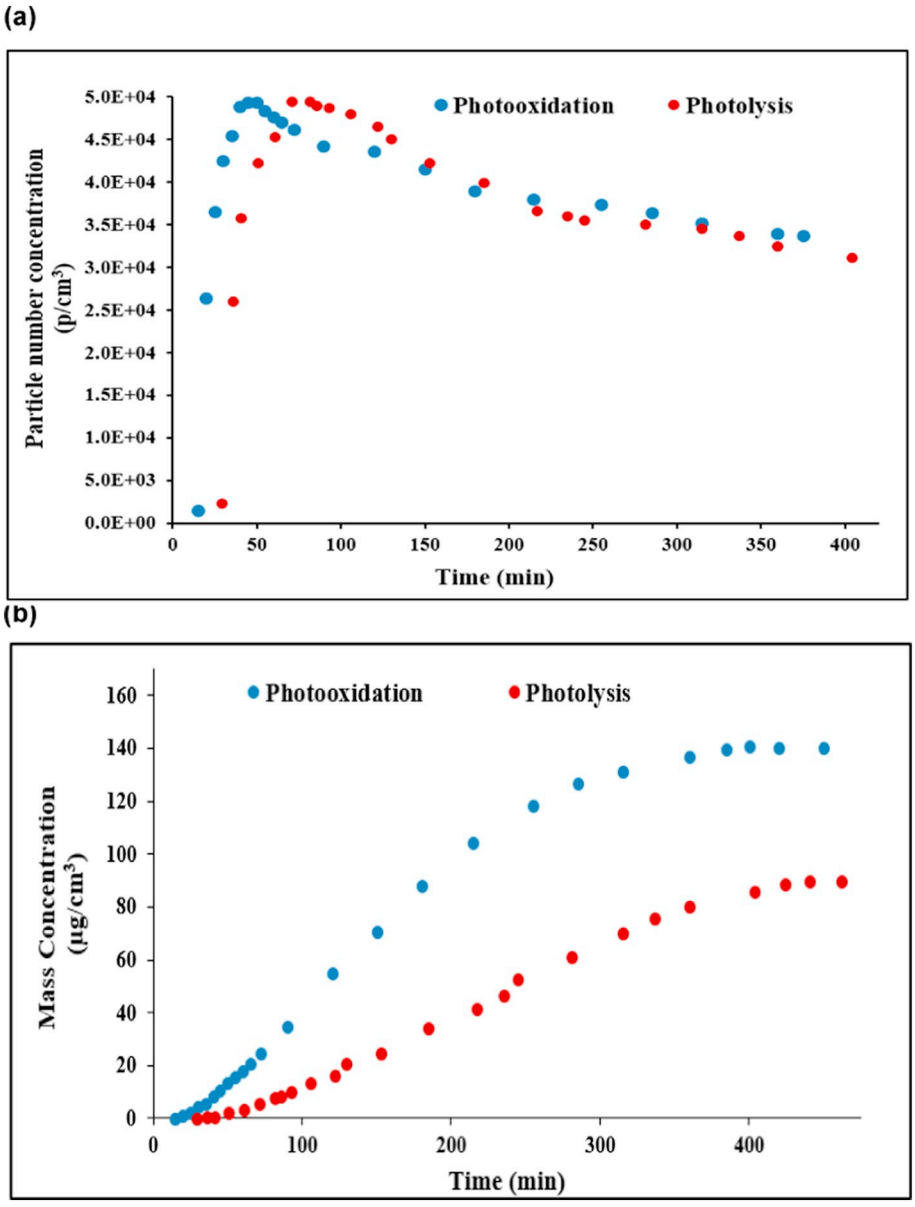

Fig. 1. Typical temporal profiles of particle number concentration (a) and SOA mass (corrected for wall-loss correction) (b) under dry conditions, low NOx and without seed particles from α-methylstyrene photolysis and photooxidation (reference experiment). Data are selected from experiments with 0.75 ppm of α-methylstyrene, in both cases, and 2 ppm of H_2O_2 for the photooxidation experiment.

discrepancies under different experimental conditions. It was found for toluene that the SOA yield decreased when RH increased for low-NOx (Cao and Jang, 2010; Hinks et al., 2018). In contrast, a positive correlation between RH and SOA yield was also observed in the presence of hygroscopic seed particles for toluene (Kamens et al., 2011), benzene and ethylbenzene (Zhou et al., 2011) and without seed for styrene (Tajuelo et al., 2019a). Finally, a non-significant effect was observed for 1,3,5-trimethylbenzene in the presence or lack of seed at 50% RH (Cocker III et al., 2001). Thus, the effect of RH in SOA formation appears to be variable.

One of the possible roles of water that would affect SOA yields is its effect in the heterogeneous formation of HONO by the reaction of NO_2 and water. This reaction is an important OH radical source in simulation chambers (Finlayson-Pitts et al., 2003; Healy et al., 2009). The increase in OH radical concentration may, in turn, increase the oxidation rate to form higher amounts of less volatile compounds that can transfer to the particle phase, thereby contributing to SOA formation (Ng et al., 2007b). This is not the case for the present work, where OH concentrations have been observed to remain practically constant in experiments with and without water. This suggests that RH has another effect on SOA yields. Water may affect the mechanism of SOA formation, chemical composition and physical properties of SOA (Seinfeld et al., 2001; Poulain et al., 2010). The observed increase of SOA yield when RH increases can be explained from the increase in SOA formation through heterogeneous reactions and aqueous chemistry in wet aerosols (Lim et al., 2010). In these atmospheric processes, aldehydes and ketones formed from the photooxidation of aromatic compounds in the gas phase can be absorbed into the humid surface of the hygroscopic SOA at high RH. This further contributes to the formation of low-volatility products on the SOA surface. Moreover, the photooxidation of aromatic compounds lead to anhydrides formation (Kautzman et al., 2010; Jia and Xu, 2014), which can hydrolyse to the corresponding acid. These new products have a lower volatility and may therefore contribute to the SOA mass yields.

With regard to experiments where the mixed effect of NOx and RH on SOA formation (high NOx experiments in wet conditions) were

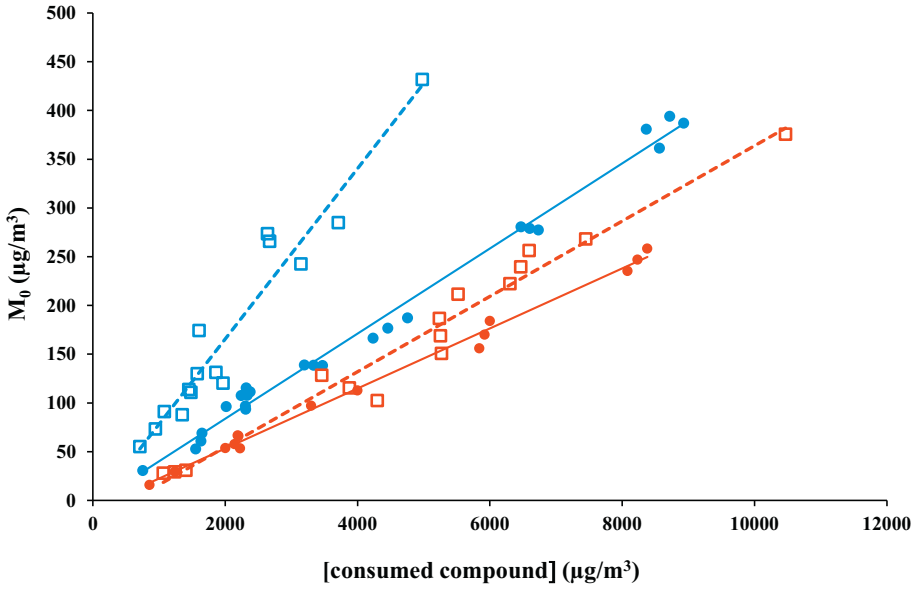

Fig. 2. SOA mass concentration (M_0) versus the consumed compound concentration, α-methylstyrene (circle) or styrene (square), measured at the end of the photolysis (red) and photooxidation (blue) experiments. (For interpretation of the references to colour in this figure legend, the reader is referred to the web version of this article.)

studied, a combined effect was observed. The SOA formation from α-methylstyrene photolysis and photooxidation in the presence of NOx was promoted at high RH, although the yields obtained were lower than those obtained without NOx.

3.4. Seed aerosol effects

The effect of two inorganic seeds, $(NH_4)_2SO_4$ and $CaCl_2$, on the formation of SOA was examined during α-methylstyrene photolysis and photooxidation at low NOx and dry conditions (< 12% RH). The SOA formation is related to pre-existing particles since seed aerosols could act as the absorption or adsorption centres of SOA formation increasing its growth. According to some authors (Lu et al., 2009; Zhang et al., 2014), the surface area is an important factor in SOA growth due to competition for SOA-forming vapour deposition between the chamber wall and the seeds. Thus, this effect is pronounced only when the surface concentration reaches a threshold value.

However, the presence of seed particles in the chamber did not favour the new particles growth within the range of seed surface area concentration used in this study (see Fig. 5). A modelling study by McVay et al. (2014) showed that the rise of the seed aerosol surface area to promote condensation of SOA-forming vapours onto seed aerosol particles may not be effective for all VOC oxidation systems. SOA mass yield depends on seed aerosol surface area only in cases where the condensation of SOA-forming vapours onto seed aerosol particles is kinetically limited (i.e. the timescale for gas–particle equilibrium is competitive with or greater than the timescale for reaction and vapour wall deposition). As in our study, in the α-pinene photooxidation with OH radicals (McVay et al., 2016) and O_3 (Nah et al., 2016), SOA growth rate and mass yields were independent of seed surface area within the range of seed surface areas tested. The characteristic timescale to establish gas–particle equilibrium is smaller than those for reaction and vapour wall deposition. When the vapour and particle phases maintain equilibrium, gas–particle equilibrium is controlled by the amount of organic matter in the VOC system. As a result, the rate of condensation of SOA-forming vapours is independent of the seed aerosol surface area (McVay et al., 2014).

3.5. Characterization of gas and particle phase products

A qualitative analysis was performed of the gas and particle phase products for photolysis and photooxidation experiments, involving the presence or absence of NOx in dry conditions. Denuder and filter extracts, which represent the gas and particle phase products respectively, were subjected to PFBHA derivatization and analysed using GC–MS.

Both in gas and particle phase, the identified products have been acetophenone, as main detected product, and acetol (Fig. S3). Both products were identified by comparing the retention times and their mass spectra with those obtained from commercial standards after PFBHA derivation (Fig. S4).

If we compare the GC–MS chromatograms obtained after derivatizing with PFBHA the filters from photolysis and photooxidation experiments, no significant differences are found under the chromatographic conditions used, except for the fact that the products peaks intensity was larger in absence of NOx (Fig. S3). During filter analysis, other products, such as benzoic acid and formaldehyde, were also searched without adding any derivatizing agent and selecting some of their characteristic *m/z* peaks, but none was detected. This could be explained in part due to smaller yields of SOA in this type of experiments.

To investigate the contribution of the main product detected, acetophenone, to the gas and particle phases, we used the set of two-dimensional volatility bases (2D-VBS) (Donahue et al., 2011), which provides correlations to estimate effective saturation concentrations based on group contribution factors and O: C oxygenation ratio. For this product, with eight carbon atoms and one oxygen atom, an effective saturation concentration of $\sim 1 \times 10^7$ µg/m^3 is predicted. Taking into account this high value, acetophenone would be in gas phase mainly, although once other organic compounds have begun to condense and an organic layer has formed on the particles, this product could partition a portion of its mass into the condensed organic phase (Pankow, 1994), as it has been observed. To the best of our knowledge, no previous studies have been carried out to characterize the particle phase products for this reaction system that can be compared with the present one. So, further experiments with an online particle analysis system would help to identify other products.

On the other hand, the presence of acetophenone, mainly in gas phase, suggests that the OH attack concerns mainly the aliphatic moiety of the aromatic molecule. This agrees with previous studies where acetophenone was identified as the majority product in the α-methylstyrene gas-phase oxidation with OH radicals and Cl atoms (Bignozzi et al., 1981; Tajuelo et al., 2019b). Moreover, in this work acetol was also identified as reaction product, which confirms that the position β is the preferred position for the OH attack, since by resonance a more stable radical is formed. Thus, in the proposed mechanism (Fig. 4), RO_2

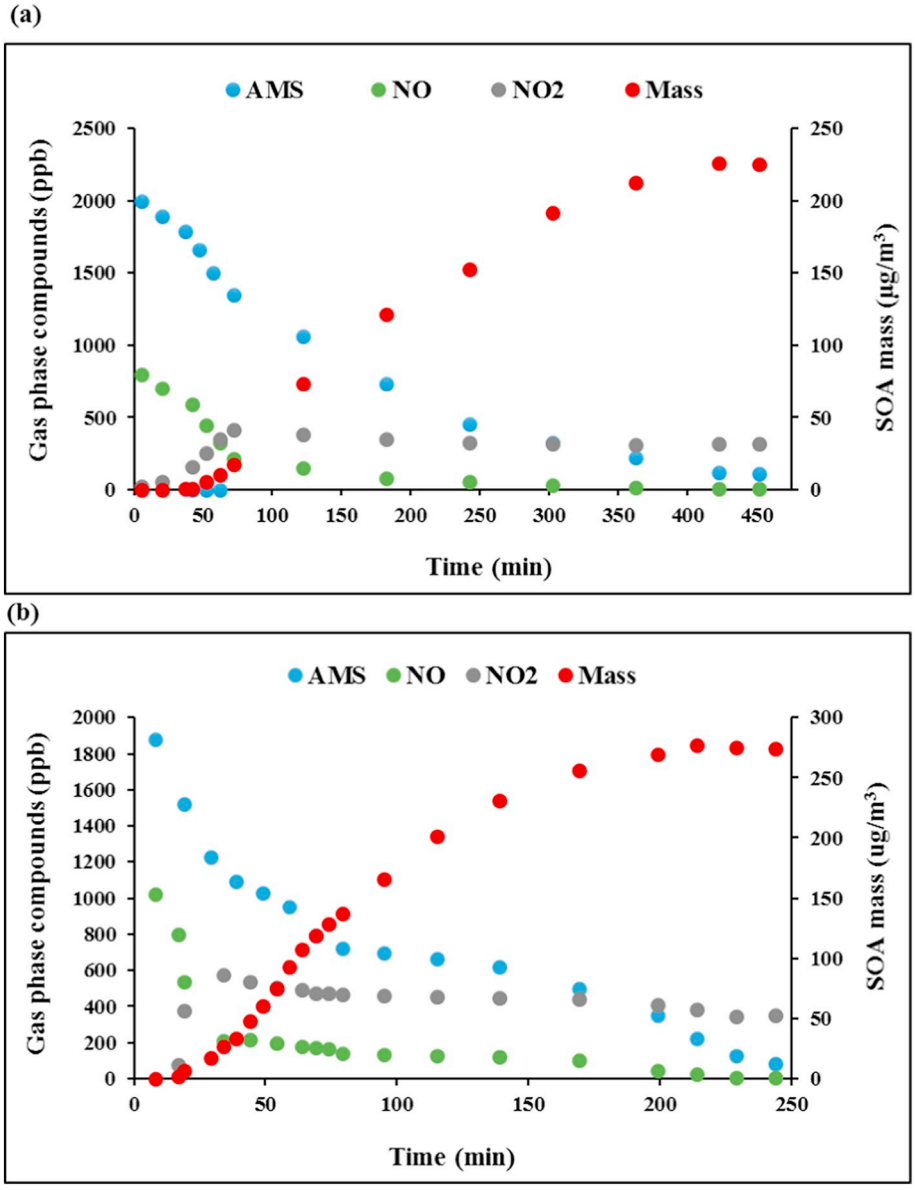

Fig. 3. Concentration-time profiles for the (a) photolysis experiment and (b) photooxidation experiment of α-methylstyrene (AMS) with high NOx concentrations (experiments type 2).

would be $C_6H_5C(CH_3)(O_2^{\cdot})CH_2(OH)$ preferably, which would lead to acetophenone and acetol mainly in gas phase after its decomposition. This result differs of that obtained for the Cl oxidation, where both carbons of the vinyl group are attacked, since Cl atoms are, in general, less discriminating than the OH radicals in their reactions with organic compounds (Tajuelo et al., 2019b).

4. Conclusions

In the present study, SOA formation from α-methylstyrene photolysis and OH-photooxidation is investigated in a simulation chamber at room temperature and atmospheric pressure. Four environmental parameters that could affect SOA yields and composition have been examined in detail: α-methylstyrene concentrations, NOx levels, RH and the presence of inorganic seed aerosols. As expected, SOA yields were higher in OH-initiated photooxidation than in photolysis, and in both processes, the organic aerosol formation can be described by a one-product gas/particle partitioning absorption model. Furthermore, the results confirmed that lower NOx concentrations and higher RH enhance SOA formation; however, seed aerosols do not affect the SOA yield both with $(NH_4)_2SO_4$ and $CaCl_2$ even when increasing the seed surface under dry conditions. Basing upon an off-line analysis of SOA composition, we found acetophenone and acetol were the only identified products under all experimental conditions studied. This result suggests that the photolysis or OH attack concerns mainly the aliphatic moiety of the α-methylstyrene, being position?β the preferred position.

It should be pointed out that the photolysis could not compete OH oxidation in the presence of longer-wavelength tropospheric radiation (e.g. $\lambda > 300$ nm), where the α-methylstyrene absorption cross section is much lower (Le Person et al., 2008). In these conditions, the OH oxidation would be the dominant process in α-methylstyrene tropospheric degradation, and hence, the atmospherically relevant SOA yield may be the difference of the photooxidation and photolysis SOA yield values obtained in this study. In this way, the atmospheric SOA yield value under dry/low-NOx conditions and 250 ppb of α-methylstyrene, the lowest compound concentration and the most representative of tropospheric conditions in this work, should be 1.0%.

Finally, it is worth noting that the concentrations of α-

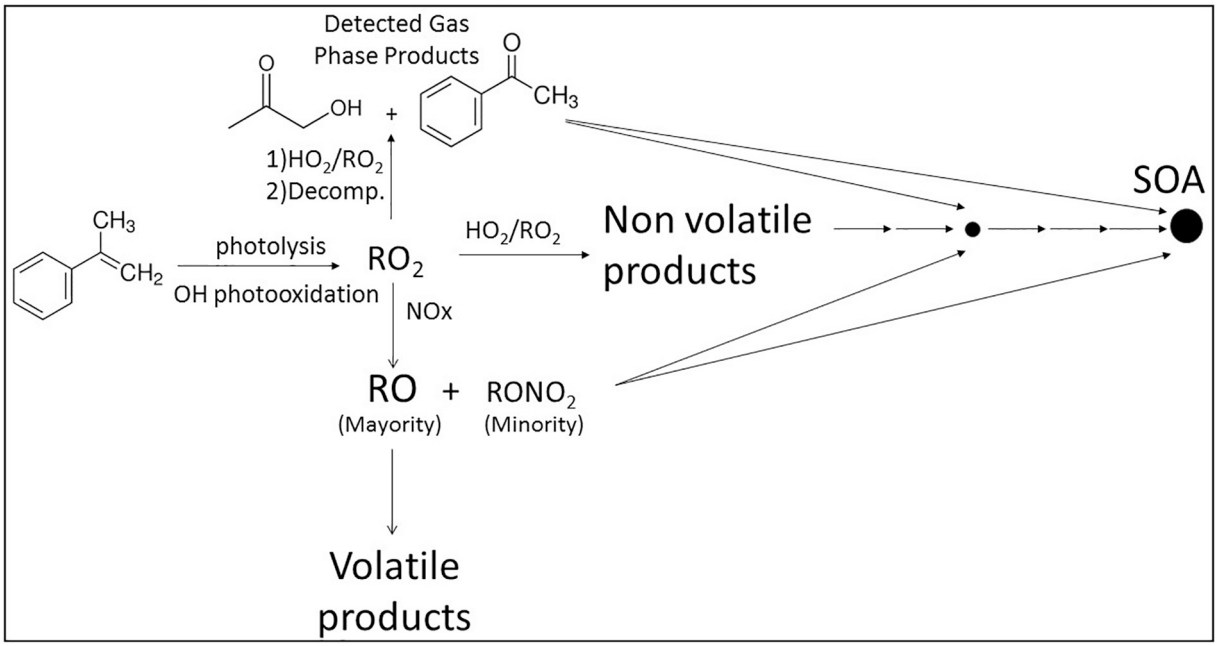

Fig. 4. Mechanism in gas and particle phase for the photolysis and OH-photooxidation of α-methylstyrene in presence and absence of NOx.

methylstyrene and NOx in our smog chamber are higher than those in the ambient atmosphere. However, the results of this study provide new information for discussing aromatic SOA formation mechanisms, which may be useful for SOA formation modelling, especially for air quality simulations of developing cities experiencing serious fine particulate matter pollution.

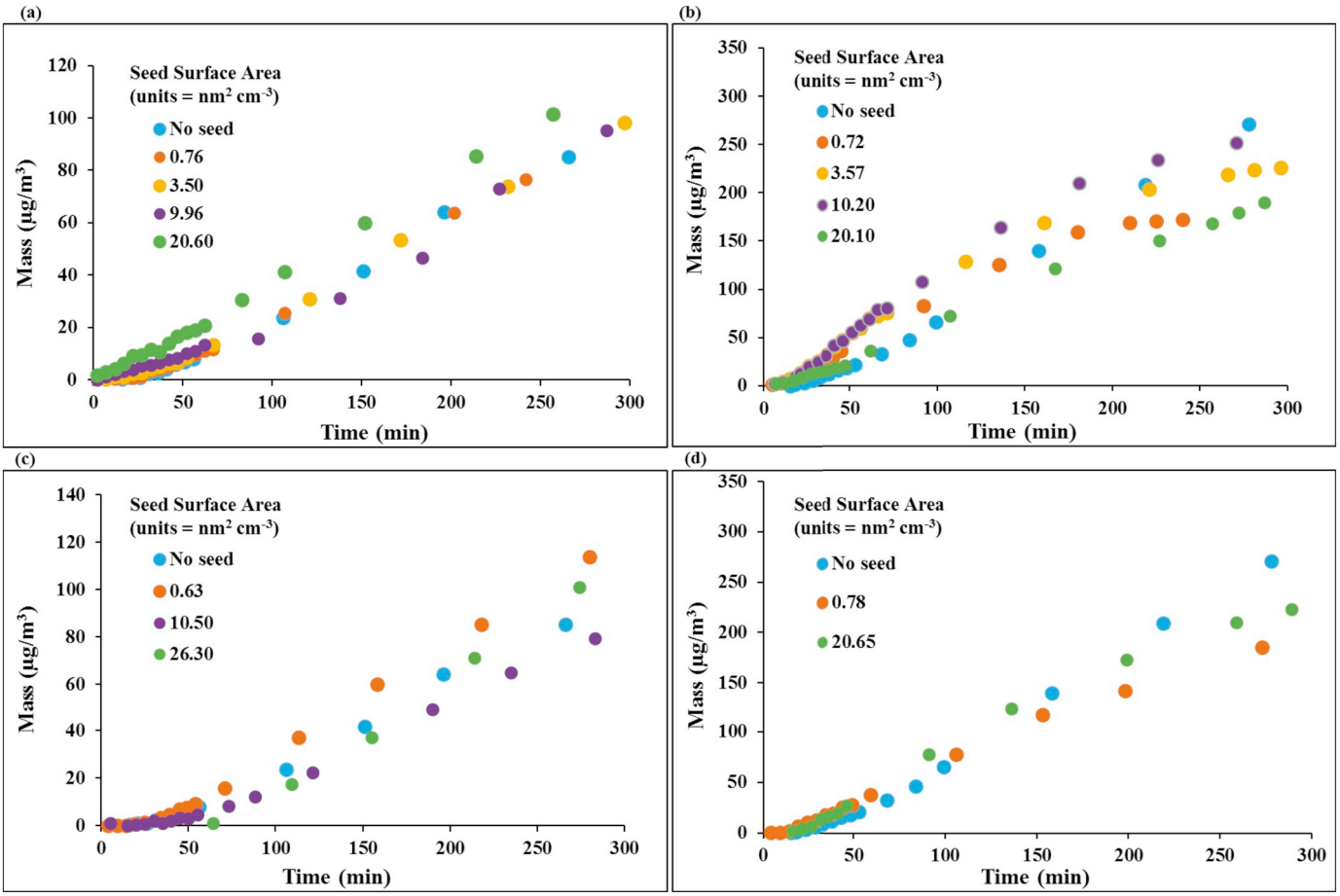

Fig. 5. Temporal evolutions of generated SOA mass in experiments with/without $(NH_4)_2SO_4$ (a: photolysis; b: photooxidation) and $CaCl_2$ (c: photolysis; d: photooxidation) seed aerosols. SOA mass is calculated subtracting the initial mass of seed aerosols to the final mass at each experiment.

Acknowledgements

This work was supported by the Spanish Ministerio de Economía y Competitividad (project CGL2014-57087-R) and by the Junta de Comunidades de Castilla-La Mancha (SBPLY/17/180501/000522).

Appendix A. Supplementary data

Supplementary data to this article can be found online at https://doi.org/10.1016/j.atmosres.2019.104631.

References

Ahmad, W., Coeur, C., Cuisset, A., Coddeville, P., Tomas, A., 2017. Effects of scavengers of Criegee intermediates and OH radicals on the formation of secondary organic aerosol in the ozonolysis of limonene. J. Aerosol Sci. 110, 70–83. https://doi.org/10.1016/j.jaerosci.2017.05.010.

Aranda, A., Diaz-de-Mera, Y., Notario, A., Rodriguez, D., Rodríguez, A., 2015. Fine and ultrafine particles in small cities. A case study in the south of Europe. Environ. Sci. Pollut. Res. 22, 18477–18486. https://doi.org/10.1007/s11356-015-5165-4.

Berezina, E.V., Moiseenko, K.B., Skorokhod, A.I., Elansky, N.F., Belikov, I.B., 2017. Aromatic volatile organic compounds and their role in ground-level ozone formation in Russia. Dokl. Earth Sci. 474, 599–603. https://doi.org/10.1134/S1028334X1705021X.

Bignozzi, C.A., Maldotti, A., Chiorboli, C., Bartocci, C., Carassiti, V., 1981. Kinetics and mechanism of reactions between aromatic olefins and hydroxyl radical. Int. J. Chem. Kinet. 13, 1235–1242. https://doi.org/10.1002/kin.550131204.

Breitner, S., Liu, L., Cyrys, J., Brüske, I., Franck, U., Schlink, U., Leitte, A.M., Herbarth, O., Wiedensohler, A., Wehner, B., Hu, M., Pan, X., Wichmann, H.E., Peters, A., 2011. Sub-micrometer particulate air pollution and cardiovascular mortality in Beijing. China. Sci. Total Environ. 409, 5196–5204. https://doi.org/10.1016/j.scitotenv.2011.08.023.

Cao, G., Jang, M., 2007. Effects of particle acidity and UV light on secondary organic aerosol formation from oxidation of aromatics in the absence of NOx. Atmos. Environ. 41, 7603–7613. https://doi.org/10.1016/j.atmosenv.2007.05.034.

Cao, G., Jang, M., 2010. An SOA model for toluene oxidation in the presence of inorganic aerosols. Environ. Sci. Technol. 44, 727–733. https://doi.org/10.1021/es901682r.

Carey, F.A., Sundberg, R.J., 2000. Advanced Organic Chemistry, Part A: Structure and Mechanisms, fourth ed. Springer Science + Business Media, Inc., USA.

Cocker III, D.R., Mader, B.T., Kalberer, M., Flagan, R.C., Seinfeld, J.H., 2001. The effect of water on gas–particle partitioning of secondary organic aerosol: II. M-xylene and 1,3,5-trimethylbenzene photooxidation systems. Atmos. Environ. 35, 6073–6085. https://doi.org/10.1016/S1352-2310(01)00405-8.

Coeur-Tourneur, C., Foulon, V., Laréal, M., 2010. Determination of aerosol yields from 3-methylcatechol and 4-methylcatechol ozonolysis in a simulation chamber. Atmos. Environ. 44, 852–857. https://doi.org/10.1016/j.atmosenv.2009.11.027.

Diaz-de-Mera, Y., Aranda, A., Martinez, E., Rodriguez, A.A., Rodriguez, D., Rodriguez, A., 2017. Formation of secondary aerosols from the ozonolysis of styrene: effect of SO_2 and H_2O.Atmos. Environ. 171, 25–31. https://doi.org/10.1016/j.atmosenv.2017.10.011.

Donahue, N.M., Epstein, S.A., Pandis, S.N., Robinson, A.L., 2011. A two-dimensional volatility basis set: 1. Organic-aerosol mixing thermodynamics. Atmos. Chem. Phys. 11, 3303–3318. https://doi.org/10.5194/acp-11-3303-2011.

Dzepina, K., Volkamer, R.M., Madronich, S., Tulet, P., Ulbrich, I.M., Zhang, Q., Cappa, C.D., Ziemann, P.J., Jimenez, J.L., 2009. Evaluation of recently-proposed secondary organic aerosol models for a case study in Mexico City. Atmos. Chem. Phys. 9, 5681–5709. https://doi.org/10.5194/acp-9-5681-2009.

Finlayson-Pitts, B.J., Wingen, L.M., Sumner, A.L., Syomin, D., Ramazan, K.A., 2003. The heterogeneous hydrolysis of NO2 in laboratory systems and in outdoor and indoor atmospheres: an integrated mechanism. Phys. Chem. Chem. Phys. 5 (2), 223–242. https://doi.org/10.1039/B208564J.

Gentner, D.R., Worton, D.R., Isaaman, G., Davis, L.C., Dallmann, T.R., Wood, E.C., Herndon, S.C., Goldstein, A.H., Harley, R.A., 2013. Chemical compositions of gas phase organic carbon emissions from motor vehicles and implications for ozone production. Environ. Sci. Technol. 47, 11837–11848. https://doi.org/10.1021/es401470e.

Gouw, J., Jimenez, J.L., 2009. Organic aerosols in the Earth's atmosphere. Environ. Sci. Technol. 43, 7614–7618. https://doi.org/10.1021/es9006004.

Hallquist, M., Wenger, J.C., Baltensperger, U., Rudich, Y., Simpson, D., Claeys, M., Dommen, J., Donahue, N.M., George, C., Goldstein, A.H., Hamilton, J.F., Herrmann, H., Hoffmann, T., Iinuma, Y., Jang, M., Jenkin, M.E., Jimenez, J.L., Kiendler-Scharr, A., Maenhaut, W., McFiggans, G., Mentel, T.F., Monod, A., Prevot, A.S.H., Seinfeld, J.H., Surratt, J.D., Szmigielski, R., Wildt, J., 2009. The formation, properties and impact of secondary organic aerosol: current and emerging issues. Atmos. Chem. Phys. 9, 5155–5523. https://doi.org/10.5194/acp-9-5155-2009.

Hand, J.L., Malm, W.C., 2007. Review of aerosol mass scattering efficiencies from ground-based measurements since 1990. J. Geophys. Res.-Atmos. 112, D16203. https://doi.org/10.1029/2007JD008484.

Healy, R.M., Temime, B., Kuprovskyte, K., Wenger, J.C., 2009. Effect of relative humidity on gas/particle partitioning and aerosol mass yield in the photooxidation of p-xylene. Environ. Sci. Technol. 43, 1884–1889. https://doi.org/10.1021/es802404z.

Hein, R., Crutzen, P.J., Heimann, M., 1997. An inverse modeling approach to investigate the global atmospheric methane cycle. Global Biogeochem. Cyc. 11, 43–76. https://doi.org/10.1029/96GB03043.

Hinks, M.L., Montoya-Aguilera, J., Ellison, L., Lin, P., Laskin, A., Laskin, J., Shiraiwa, M., Dabdub, D., Nizkorodov, S.A., 2018. Effect of relative humidity on the composition of secondary organic aerosol from the oxidation of toluene. Atmos. Chem. Phys. 18, 1643–1652. https://doi.org/10.5194/acp-18-1643-2018.

NTP (National Toxicology Programa), 2007. Technical report on the toxicology and carcinogenesis studies of α-methylstyrene (CAS NO. 98-83-9) in F344/N rats AND B6C3F1 mice (inhalation studies). Natl. Toxicol. Program. Tech. 543, 1–210. https://ntp.niehs.nih.gov/ntp/htdocs/lt_rpts/tr543.pdf.

Huang, M., Hao, L., Cai, S., Gu, X., Zhang, W., Hu, C., Wang, Z., Fang, L., Zhang, W., 2017. Effects of inorganic seed aerosols on the particulate products of aged 1,3,5-trimethylbenzene secondary organic aerosol. Atmos. Environ. 152, 490–502. https://doi.org/10.15244/pjoes/66768.

IARC (International Agency of Research for Cancer), 2019. Agents Classified by the IARC Monographs. Vol. 1–123. https://monographs.iarc.fr/agents-classified-by-the-iarc/ (Last update 25 March 2019).

Jia, L., Xu, Y., 2010. Formation of secondary organic aerosol from the styrene-NO*x* irradiation. Acta Chim. Sin. 68, 2429–2435.

Jia, L., Xu, Y., 2014. Effects of relative humidity on ozone and secondary organic aerosol formation from the photooxidation of benzene and ethylbenzene. Aerosol Sci. Technol. 48, 1–12. https://doi.org/10.1080/02786826.2013.847269.

Johnson, D., Jenkin, M.E., Wirtz, K., Martin-Reviejo, M., 2005. Simulating the formation of secondary organic aerosol from the photooxidation of aromatic hydrocarbons. Environ. Chem. 2, 35–48. https://doi.org/10.1071/EN04079.

Kamens, R.M., Zhang, H., Chen, E.H., Zhou, Y., Parikh, H.M., Wilson, R.L., Galloway, K.E., Rosen, E.P., 2011. Secondary organic aerosol formation from toluene in an atmospheric hydrocarbon mixture: water and particle seed effects. Atmos. Environ. 45, 2324–2334. https://doi.org/10.1016/j.atmosenv.2010.11.007.

Kanakidou, M., Seinfeld, J.H., Pandis, S.N., Barnes, I., Dentener, F.J., Facchini, M.C., Van Dingenen, R., Ervens, B., Nenes, A., Nielsen, C.J., Swietlicki, E., Putaud, J.P., Balkanski, Y., Fuzzi, S., Horth, J., Moortgat, G.K., Winterhalter, R., Myhre, C.E.L., Tsigaridis, K., Vignati, E., Stephanou, E.G., Wilson, J., 2005. Organic aerosol and global climate modelling: a review. Atmos. Chem. Phys. 5, 1053–1123. https://doi.org/10.5194/acp-5-1053-2005.

Kautzman, K.E., Surratt, J.D., Chan, M.N., Chan, A.W.H., Hersey, S.P., Chhabra, P.S., Dalleska, N.F., Wennberg, P.O., Flagan, R.C., Seinfeld, J.H., 2010. Chemical composition of gas- and aerosol-phase products from the photooxidation of naphthalene. J. Phys. Chem. A 114, 913–934. https://doi.org/10.1021/jp908530s.

Kleindienst, T.E., Jaoui, M., Lewandowski, M., Offenberg, J.H., Docherty, K.S., 2012. The formation of SOA and chemical tracer compounds from the photooxidation of naphthalene and its methyl analogs in the presence and absence of nitrogen oxides. Atmos. Chem. Phys. 12, 8711–8726. https://doi.org/10.5194/acp-12-8711-2012.

Knighton, W.B., Herndon, S.C., Wood, E.C., Fortner, E.C., Onasch, T.B., Wormhoudt, J., Kolb, C.E., Lee, B.H., Zavala, M., Molina, L., Jones, M., 2012. Detecting fugitive emissions of 1,3-butadiene and styrene from a petrochemical facility: an application of a mobile laboratory and a modified proton transfer reaction mass spectrometer. Ind. Eng. Chem. Res. 51, 12706–12711. https://doi.org/10.1021/ie202794j.

Kroll, J.H., Seinfeld, J.H., 2008. Chemistry of secondary organic aerosol: formation and evolution of low-volatility organics in the atmosphere. Atmos. Environ. 42, 3593–3624. https://doi.org/10.1016/j.atmosenv.2008.01.003.

Kroll, J.H., Ng, N.L., Murphy, S.M., Flagan, R.C., Seinfeld, J.H., 2006. Secondary organic aerosol formation from isoprene photooxidation. Environ. Sci. Technol. 40, 1869–1877. https://doi.org/10.1021/es0524301.

Lauraguais, A., Coeur-Tourneur, C., Cassez, A., Seydi, A., 2012. Rate constant and secondary organic aerosol yields for the gas-phase reaction of hydroxyl radicals with syringol (2,6-dimethoxyphenol). Atmos. Environ. 55, 43–48. https://doi.org/10.1016/j.atmosenv.2012.02.027.

Le Person, A., Eyglunent, G., Daële, V., Mellouki, A., Mu, Y., 2008. The near UV absorption cross-sections and the rate coefficients for the ozonolysis of a series of styrene-like compounds. J. Photochem. Photobiol. A 195, 54–63. https://doi.org/10.1016/j.jphotochem.2007.09.006.

Lewandowski, M., Jaoui, M., Offenberg, J.H., Kleindienst, T.E., Edney, E.O., Sheesley, R.J., Schauer, J.J., 2008. Primary and secondary contributions to ambient PM in the midwestern United States. Environ. Sci. Technol. 42, 3303–3309. https://doi.org/10.1021/es0720412.

Lewis, P., Hagopian, C., Koch, P., 1983. Styrene. In: Grayson, M., Eckroth, D. (Eds.), Kirk-Othmer Encyclopedia of Chemical Technology, 3rd ed. Vol. 21. John Wiley & Sons, New York, pp. 770–801.

Li, K., Wang, W., Ge, M., Li, J., Wang, D., 2014. Optical properties of secondary organic aerosols generated by photooxidation of aromatic hydrocarbons. Sci. Rep. 4, 4922. https://doi.org/10.1038/srep04922.

Li, P., Tang, S., Nakao, D.R., Cocker, I.I.I., 2016. Impact of molecular structure on secondary organic aerosol formation from aromatic hydrocarbon photooxidation under low-NOx conditions. Atmos. Chem. Phys. 16, 10793–10808. https://doi.org/10.5194/acp-16-10793-2016.

Lim, Y.B., Tan, Y., Perri, M.J., Seitzinger, S.P., Turpin, B.J., 2010. Aqueous chemistry and its role in secondary organic aerosol (SOA) formation. Atmos. Chem. Phys. 10, 10521–10539. https://doi.org/10.5194/acp-10-10521-2010.

Liu, C., Liu, Y., Chen, T., Liu, J., He, H., 2019. Rate constant and secondary organic aerosol formation from the gas-phase reaction of eugenol with hydroxyl radicals. Degradation kinetics and secondary organic aerosol formation from eugenol by hydroxyl radicals. Atmos. Chem. Phys. 19, 2001–2013. https://doi.org/10.5194/acp-2018-749.

Lu, Z., Hao, J., Takekawa, H., Hu, L., Li, J., 2009. Effect of high concentrations of inorganic seed aerosols on secondary organic aerosol formation in the m-xylene/NOx

photooxidation system. Atmos. Environ. 43, 897–904. https://doi.org/10.1016/j.atmosenv.2008.10.047.
McVay, R.C., Cappa, C.D., Seinfeld, J.H., 2014. Vapor–wall deposition in chambers: theoretical considerations. Environ. Sci. Technol. 48, 10251–10258. https://doi.org/10.1021/es502170j.
McVay, R.C., Zhang, X., Aumont, B., Valorso, R., Camredon, M., La, Y.S., Wennberg, P.O., Seinfeld, J.H., 2016. SOA formation from the photooxidation of α-pinene: systematic exploration of the simulation of chamber data. Atmos. Chem. Phys. 16, 2785–2802. https://doi.org/10.5194/acp-16-2785-2016.
Nah, T., McVay, R.C., Zhang, X., Boyd, C.M., Seinfeld, J.H., Ng, N.L., 2016. Influence of seed aerosol surface area and oxidation rate on vapor wall deposition and SOA mass yields: a case study with pinene ozonolysis. Atmos. Chem. Phys. 16, 9361–9379. https://doi.org/10.5194/acp-16-9361-2016.
Nah, T., McVay, R.C., Pierce, J.R., Seinfeld, J.H., Ng, N.L., 2017. Constraining uncertainties in particle-wall deposition correction during SOA formation in chamber experiments. Atmos. Chem. Phys. 17, 2297–2310. https://doi.org/10.5194/acp-17-2297-2017.
Ng, N.L., Kroll, J.H., Keywood, M.D., Bahreini, R., Varutbangkul, V., Goldstein, A.H., 2006. Contribution of first- versus second-generation products to secondary organic aerosols formed in the oxidation of biogenic hydrocarbons. Environ. Sci. Technol. 40, 2283–2297. https://doi.org/10.1021/es052269u.
Ng, N.L., Chhabra, P.S., Chan, A.W.H., Surratt, J.D., Kroll, J.H., Kwan, A.J., McCabe, D.C., Wennberg, P.O., Sorooshian, A., Murphy, S.M., Dalleska, N.F., Flagan, R.C., Seinfeld, J.H., 2007a. Effect of NO(x) level on secondary organic aerosol (SOA) formation from the photooxidation of terpenes. Atmos. Chem. Phys. 7, 5159–5174. https://doi.org/10.5194/acp-7-5159-2007.
Ng, N.L., Kroll, J.H., Chan, A.W.H., Chhabra, P.S., Flagan, R.C., Seinfeld, J.H., 2007b. Secondary organic aerosol formation from m-xylene, toluene, and benzene. Atmos. Chem. Phys. 7, 3909–3922. https://doi.org/10.5194/acp-7-3909-2007.
Odum, J.R., Hoffmann, T., Bowman, F., Collins, D., Flagan, R.C., Seinfeld, J.H., 1996. Gas/particle partitioning and secondary organic aerosol yields. Environ. Sci. Technol. 30, 2580–2585. https://doi.org/10.1021/es950943þ.
Okada, Y., Nakagoshi, A., Tsurukawa, M., Matsumura, C., Eiho, J., Nakano, T., 2012. Environmental risk assessment and concentration trend of atmospheric volatile organic compounds in Hyogo Prefecture. Japan. Environ. Sci. Pollut. Res. 19, 201–213. https://doi.org/10.1007/s11356-011-0550-0.
Pankow, J.F., 1994. An absorption model of the gas/aerosol partitioning involved in the formation of secondary organic aerosol. Atmos. Environ. 28A, 189–193. https://doi.org/10.1021/es950943+.
Pope, C.A., Dockery, D.W., 2006. Health effects of fine particulate air pollution: lines that connect. J. Air Waste Manage. Assoc. 56, 709–742. https://doi.org/10.1080/10473289.2006.10464485.
Poulain, L., Wu, Z., Petters, M.D., Wex, H., Hallbauer, E., Wehner, B., Massling, A., Kreidenweis, S.M., Stratmann, F., 2010. Towards closing the gap between hygroscopic growth and CCN activation for secondary organic aerosols – part 3: influence of the chemical composition on the hygroscopic properties and volatile fractions of aerosols. Atmos. Chem. Phys. 10, 3775–3785. https://doi.org/10.5194/acp-10-3775-2010.
Presto, A.A., Hartz, K.E.H., Donahue, N.M., 2005. Secondary organic aerosol production from terpene ozonolysis 2. Effect of NOx concentration. Environ. Sci. Technol. 39, 7046–7054. https://doi.org/10.1021/es050400s.
Santodonato, J., Meylan, W.M., Davis, L.N., Howard, P.H., Orzel, D.M., Bogyo, D.A., 1980. Investigation of selected potential environmental contaminants: styrene, ethylbenzene, and related compounds, 4–228. In: Syracuse Research Corporation Report to the U.S. Environmental Protection Agency, Office of Toxic Substances. EPA Report No. 560/11–80 – 018.
Sarrafzadeh, M., Wildt, J., Pullinen, I., Springer, M., Kleist, E., Tillmann, R., Schmitt, S.H., Wu, C., Mentel, T.F., Zhao, D., Hastie, D.R., Kiendler-Scharr, A., 2016. Impact of NO_x and OH on secondary organic aerosol formation from β-pinene photooxidation. Atmos. Chem. Phys. 16, 11237–11248. https://doi.org/10.5194/acp-16-11237-2016.
Seinfeld, J.H., Erdakos, G.B., Asher, W.E., Pankow, J.F., 2001. Modeling the formation of secondary organic aerosol (SOA). 2. The predicted effects of relative humidity on aerosol formation in the r-Pinene-, â-Pinene-, Sabinene-, ¢3-Carene-, and Cyclohexene-ozone systems. Environ. Sci. Technol. 35, 1806–1817. https://doi.org/10.1021/es001765+.
Song, C., Na, K., Cocker III, D.R., 2005. Impact of the hydrocarbon to NOx ratio on secondary organic aerosol formation. Environ. Sci. Technol. 39, 3143–3149. https://doi.org/10.1021/es0493244.
Song, C., Zaveri, R.A., Alexander, M.L., Thornton, J.A., Madronich, S., Ortega, J.V., Zelenyuk, A., Yu, X.Y., Laskin, A., Maughan, D.A., 2007. Effect of hydrophobic primary organic aerosols on secondary organic aerosol formation from ozonolysis of alpha-pinene. Geophys. Res. Lett. 34, L20803. https://doi.org/10.1029/2007GL030720.
Stocker, T.F., Qin, D., Plattner, G.K., Tignor, M., Allen, S.K., Boschung, J., Nauels, A., Xia, Y., Bex, V., Midgley, P.M., 2013. Climate change 2013: the physical science basis. In: Contribution of Working Group I to the Fifth Assessment Report of the Intergovernmental Panel on Climate Change, (Eds.). Cambridge University Press, Cambridge, UK and New York, USA.
Tajuelo, M., Rodríguez, D., Baeza-Romero, M.T., Díaz-de-Mera, Y., Aranda, A., Rodríguez, A., 2019a. Secondary organic aerosol formation from styrene photolysis and photooxidation with hydroxyl radicals. Chemosphere. 231https://doi.org/10.1016/j.chemosphere.2019.05.136. 2796–286.
Tajuelo, M., Bravo, I., Rodríguez, A., Aranda, A., Diaz-de-Mera, Y., Rodríguez, D., 2019b. Atmospheric sink of styrene, α-methylstyrene, trans-β-methylstyrene and indene: rate constants and mechanisms of Cl atom-initiated degradation. Atmos. Environ. 200, 78–89. https://doi.org/10.1016/j.atmosenv.2018.11.059.
Wang, Y., Zhuang, G., Sun, Y., An, Z., 2006. The variation of characteristics and formation mechanisms of aerosols in dust, haze, and clear days in Beijing. Atmos. Environ. 40, 6579–6591. https://doi.org/10.1016/j.atmosenv.2006.05.066.
Yuan, B., Hu, W.W.M., Shao, M., Wang, M., Chen, W.T., Lu, S.H., Zeng, L.M., Hu, M., 2013. VOC emissions, evolutions and contributions to SOA formation at a receptor site in eastern China. Atmos. Chem. Phys. 13, 8815–8832. https://doi.org/10.5194/acp-13-8815-2013.
Zhang, Q., Jimenez, J.L., Canagaratna, M.R., Allan, J.D., Coe, H., Ulbrich, I., Alfarra, M.R., Takami, A., Middlebrook, A.M., Sun, Y.L., Dzepina, K., Dunlea, E., Docherty, K., De-Carlo, P.F., Salcedo, D., Onasch, T., Jayne, J.T., Miyoshi, T., Shimono, A., Hatakeyama, S., Takegawa, N., Kondo, Y., Schneider, J., Drewnick, F., Borrmann, S., Weimer, S., Demerjian, K., Williams, P., Bower, K., Bahreini, R., Cottrell, L., Griffin, R.J., Rautianinen, J., Sun, J.Y., Zhang, Y.M., Worsnop, D.R., 2007. Ubiquity and dominance of oxygenated species in organic aerosols in anthropogenically-influenced Northern Hemisphere midlatitudes. Geophys. Res. Lett. 34, L13801. https://doi.org/10.1029/2007GL029979.
Zhang, H., Lin, Y., Zhang, Z., Zhang, X., Shaw, S.L., Knipping, E.M., Weber, R.J., Gold, A., Kamens, R.M., Surratt, J.D., 2012. Secondary organic aerosol formation from methacrolein photooxidation: roles of NOx level, relative humidity and aerosol acidity. Environ. Chem. 9, 247–262. https://doi.org/10.1071/EN12004.
Zhang, X., Cappa, C.D., Jathar, S.H., McVay, R.C., Ensberg, J.J., Kleeman, M.J., Seinfeld, J.H., 2014. Influence of vapor wall loss in laboratory chambers on yields of secondary organic aerosol. P. Natl. Acad. Sci. USA. 111, 5802–5807. https://doi.org/10.1073/pnas.1404727111.
Zhang, Z., Wang, H., Chen, D., Li, Q., Thai, P., Gong, D., Li, Y., Zhang, C., Gu, Y., Zhou, L., Morawska, L., Wang, B., 2017. Emission characteristics of volatile organic compounds and their secondary organic aerosol formation potentials from a petroleum refinery in Pearl River Delta. China. Sci. Total Environ. 15, 1162–1174. https://doi.org/10.1016/j.scitotenv.2017.01.179.
Zhou, Y., Zhang, H., Parikh, H.M., Chen, E.H., Rattanavaraha, W., Rosen, E.P., Wang, W., Kamens, R.M., 2011. Secondary organic aerosol formation from xylenes and mixtures of toluene and xylenes in an atmospheric urban hydrocarbon mixture: Water and particle seed effects (II). Atmos. Environ. 45, 3882–3890. https://doi.org/10.1016/j.atmosenv.2010.12.048.